

Mechanical stratigraphic controls on natural fracture spacing and penetration



Ronald N. McGinnis^{a,*}, David A. Ferrill^a, Alan P. Morris^a, Kevin J. Smart^a,
Daniel Lehrmann^b

^a Department of Earth, Material, and Planetary Sciences, Southwest Research Institute, 6220 Culebra Road, San Antonio, TX 78238-5166, USA

^b Geoscience Department, Trinity University, One Trinity Place, San Antonio, TX 78212, USA

ARTICLE INFO

Article history:

Received 20 July 2016

Received in revised form

21 December 2016

Accepted 7 January 2017

Available online 8 January 2017

Keywords:

Mechanical stratigraphy

Natural fractures

Fracture spacing

Fracture penetration

ABSTRACT

Fine-grained low permeability sedimentary rocks, such as shale and mudrock, have drawn attention as unconventional hydrocarbon reservoirs. Fracturing – both natural and induced – is extremely important for increasing permeability in otherwise low-permeability rock. We analyze natural extension fracture networks within a complete measured outcrop section of the Ernst Member of the Boquillas Formation in Big Bend National Park, west Texas. Results of bed-center, dip-parallel scanline surveys demonstrate nearly identical fracture strikes and slight variation in dip between mudrock, chalk, and limestone beds. Fracture spacing tends to increase proportional to bed thickness in limestone and chalk beds; however, dramatic differences in fracture spacing are observed in mudrock. A direct relationship is observed between fracture spacing/thickness ratio and rock competence. Vertical fracture penetrations measured from the middle of chalk and limestone beds generally extend to and often beyond bed boundaries into the vertically adjacent mudrock beds. In contrast, fractures in the mudrock beds rarely penetrate beyond the bed boundaries into the adjacent carbonate beds. Consequently, natural bed-perpendicular fracture connectivity through the mechanically layered sequence generally is poor. Fracture connectivity strongly influences permeability architecture, and fracture prediction should consider thin bed-scale control on fracture heights and the strong lithologic control on fracture spacing.

© 2017 Elsevier Ltd. All rights reserved.

1. Introduction

In geology, a fracture is any discontinuity in the rock where cohesion has been lost via a brittle deformation process (Price, 1966; Ramsay, 1967; Hancock, 1985; Ramsay and Huber, 1987). Most rocks are fractured at some scale (micro-, meso-, or macro-scale), and all scales and types of fractures (i.e., faults, opening-mode fractures [barren and vein filled], and stylolites) impact how fluid moves through rock. Fractures can enhance permeability in otherwise impermeable rocks, or conversely decrease permeability by acting as barriers, or compartmentalize blocks of rock and create permeability anisotropy. Accurate determinations of the presence, size (vertical and lateral trace lengths), orientation, spacing, and aperture of natural fracture types and sets are essential to characterizing permeability architecture. In the subsurface, natural fracture data are often interpreted from ambiguous datasets

(microseismic data, two- and three-dimensional seismic reflection data, wellbore formation microimager, oil-based mud imager, and core), predicted using published relationships, modeled from low-resolution data, and quite often have very different fracture patterns compared to outcrop analogs of the same rock. Direct application of these methods may produce an incomplete or inaccurate representation of the actual fracture system. Natural and induced fractures are subject to controls imposed by mechanical stratigraphy, structural position and timing with respect to other natural deformation features (such as faults and folds), and *in situ* stress conditions (Engelder, 1985; Hancock, 1985; Ferrill et al., 2014). Focusing on the mechanisms that control natural fracture development can improve fracture characterizations.

Using consistent approaches and terminology for fracture analyses is important. However, many times the observations and relationships derived from a particular study are only relevant to a particular system and not necessarily useful for application to other systems. Fracture characterization approaches, terminology, and relationships must be screened for usefulness and relevance prior to

* Corresponding author.

E-mail address: rmcginnis@swri.org (R.N. McGinnis).

their application. For example, in the subsurface where data is too coarse to perform a detailed analysis of fracture type, distribution (by type), vertical and lateral penetration, and spacing of properly grouped fracture type (e.g., vein, barren, shear, hybrid, tensile) and orientation (e.g., fracture set), it is important to assess likely conditions at the time of fracturing and to select relevant analogs and fracture prediction approaches that will lead to defensible fracture interpretations and predictions. Thorough characterization of mechanical stratigraphy is a fundamental factor that should be considered in selecting relevant analogs and fracture prediction approaches.

In this study, we examine the controls on fracture spacing and vertical penetration in mechanically layered strata of the Late Cretaceous Ernst Member of the Boquillas Formation exposed at Ernst Tinaja within the Sierra del Carmen in west Texas (Fig. 1).

The Ernst Member is the lateral equivalent of the Eagle Ford Formation, which is a major unconventional hydrocarbon source and reservoir in south Texas. Observations from three lithostratigraphic groups that include limestone, chalk, and mudrock show variations in fracture penetration and fracture spacing. We show that fracture size and distribution vary as a function of mechanical stratigraphy, and that understanding this relationship can improve fracture characterization and prediction in the subsurface.

2. Background

Careful characterization and analysis of fracture systems is necessary for understanding the natural variability of fracture networks and to ascertain the controls on fracture development

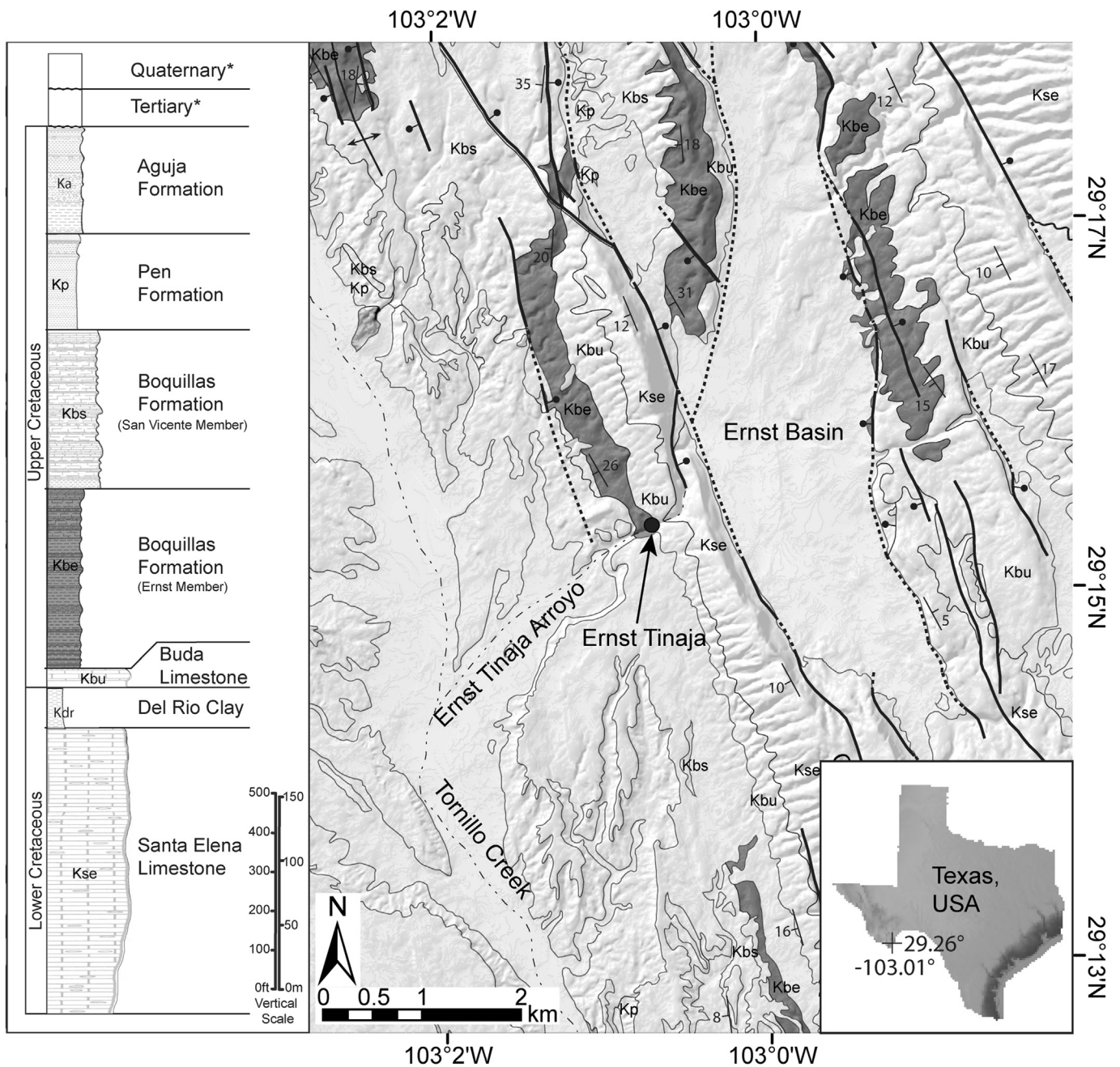


Fig. 1. Geologic map and stratigraphic section modified from Ferrill et al. (2016). The map shows the location of Ernst Tinaja and the dark grey formation (focus of this study) is the outcrop of the Ernst Member of the Boquillas Formation. The stratigraphic section is based on thicknesses from measured sections found in Maxwell et al. (1967).

(e.g., Narr, 1991; Gross, 1993; Gillespie et al., 2001; Nelson, 2001; Narr et al., 2006; Olson et al., 2009; Laubach et al., 2009, 2010; Ortega et al., 2010; English, 2012; Hooker et al., 2013; Gale et al., 2014; McGinnis et al., 2015). However, in the subsurface where data is sparse, noisy, or unreliable, information derived from outcrop studies can be critical to help constrain fracture characterization, interpretation, and prediction. There can be significant variability from one set of rocks to another that depends on a host of factors, and isolating the influence of individual factors, such as bed thickness and mechanical properties of layers, is important for enhancing the usefulness and reducing the uncertainty in fracture prediction techniques.

Deformation style (fault, fold, opening-mode fracture, stylolite), failure type (tensile, hybrid, and shear), and fracture frequency are highly sensitive to mechanical stratigraphy (for example, Corbett et al., 1987; Ferrill and Morris, 2008; Laubach et al., 2009; Ferrill et al., 2014, 2017; McGinnis et al., 2015, 2016). Ferrill et al. (2017) describe mechanical stratigraphy as encompassing (i) the varying material properties of rock strata (e.g., measured properties such as compressive and tensile strengths, Young's moduli), (ii) thicknesses of the mechanical layers, and (iii) the character and frictional properties of the transitions or boundaries between mechanical layers (e.g., sharp formation or bed contacts versus gradational boundaries, and smooth or planar contacts versus rugose or sutured contacts) (cf., Groshong, 2006; Ferrill and Morris, 2008; Laubach et al., 2009).

Variations in stiffness and strength in heterolithic rock sequences impose distinct controls on natural and induced fracture development. A thorough, site-specific characterization of mechanical stratigraphy includes quantifying the ratio of incompetent to competent bed thickness (*i/c* ratio; Ferrill and Morris, 2008), description of layer to layer transitions (e.g., gradational versus abrupt, smooth versus undulatory, rugose or sutured), and dominant versus conforming mechanical units (Ferrill et al., 2017). With a robust characterization of the mechanical stratigraphy, it is possible to identify potential nucleation points of fractures, potential zones where fracture angle may experience refraction, likely locations for fault related folding, and anticipate failure mode transitions along a fracture.

3. Study site

3.1. Tectonic setting

The deformation observed in the Cretaceous stratigraphic section at Ernst Tinaja has experienced two nearly co-directional tectonic events, (1) northeast-southwest-directed contraction due to the Laramide orogeny (ca. 70 to 50 Ma) followed by (2) northeast-southwest-directed extension caused by the Basin and Range tectonics (ca. 25 to 2 Ma; Maxwell et al., 1967; Moustafa, 1988; Lehman, 1991; Turner et al., 2011). Contractive deformation is manifest by large-scale contractional folds and faults (Maxwell et al., 1967; Turner et al., 2011), and mesoscopic structures, including small-scale thrust faults, contractional folds, veins, tectonic stylolites, and microscale contractional deformation (Moustafa, 1988; Maler, 1990; Erdlac, 1994; Ferrill et al., 2016). Following Laramide contraction, the onset of Basin and Range extension developed a normal-faulting stress regime that produced normal faults at a wide range of scales, as well as opening-mode extension fractures including barren and vein filled and reactivated stylolites as opening-mode fractures.

3.2. Ernst Tinaja

The Ernst Tinaja arroyo is a dry wash that cuts a west dipping (~15°) homocline (cuesta) in the footwall of an east-dipping normal

fault system in the eastern part of Big Bend National Park, Texas. The dry wash cuts the homocline at a low point coincident with a breached relay ramp between two fault segments of the east-dipping fault system that forms the Ernst Basin half graben. A traverse from west to east along the dry wash passes down stratigraphic section through Cretaceous rocks of the San Vicente Member (Austin Chalk lateral equivalent) and Ernst Member (Eagle Ford lateral equivalent) of the Boquillas Formation (Turonian), and the Buda Formation (Cenomanian). The Ernst Tinaja exposure contains lithologically controlled extensional and contractional deformation features, such as opening-mode extension fractures (barren and vein filled), tectonic stylolites, tectonic stylolites that have locally reactivated to host co-planar opening-mode fractures (barren and vein filled), normal faults, thrust or “wedge” faults, bedding-plane slip surfaces, box folds, contractional and extensional fault-propagation folds (Ferrill et al., 2016).

3.2.1. Lithostratigraphy

The complete lithostratigraphy of the Ernst Tinaja exposure was measured, described, and sampled in the field using standard field tools that include Jacobs staff, measuring tape, and hand lens. The stratigraphic section at Ernst Tinaja was measured to be 110.6 m. The measured section extends from the Buda Formation at the base, through the entire Ernst Member of the Boquillas Formation, and into the San Vicente Member of the Boquillas Formation. The section includes 1.5 m of the uppermost Buda Formation, 83.9 m of the Ernst Member of the Boquillas Formation, which is the equivalent of the Eagle Ford Formation (Maxwell et al., 1967), and 25.2 m of the lower part of the San Vicente Member of the Boquillas Formation, which is the equivalent of the Austin Chalk (Maxwell et al., 1967).

The fracture analysis was performed entirely in the Ernst Member of the Boquillas Formation. The Ernst Member is a deep-marine, predominantly pelagic succession of calcareous mudrock, nannoplankton and pelagic foraminifer microgranular packstone (chalk), heterolithic thinly bedded and intercalated calcareous mudrock and limestone layers, with intervals of hydrodynamically agitated skeletal and planktonic foraminifer lime grainstone-packstone beds, and numerous volcanic ash layers. Much of the Ernst Member consists of a highly rhythmic or cyclic alternation of calcareous mudrock and chalk with gradational bedding contacts. Calcareous mudrock intervals range from 0.03 to 2.5 m with an average of 0.28 m. Chalk beds range from 0.02 to 0.96 m, with an average of 0.26 m. Hydrodynamic packstone-grainstone beds are lenticular to continuous, contain ripple cross-lamination, hummocky cross stratification, and fragmented skeletal material, and are winnowed indicating storm agitation on the seafloor. Small sections within the Ernst Member consist of hydrodynamic packstone-grainstone beds that range from 0.01 to 0.40 m, with average bed thickness of 0.11 m. Heterolithic intervals of thin-bedded intercalated intervals of mudrock and thin limestone are associated with hydrodynamic grainstone-packstone intervals that also indicate storm agitation of the seafloor – these intervals range from 0.034 to 0.48 m thick. Because of the abrupt changes in hydrodynamic regime associated with storm events, the bedding boundaries within the hydrodynamic packstone-grainstone and heterolithic facies are sharp. Volcanic ash beds occur throughout the succession and range from 0.01 to 0.16 m thick.

3.3. Timing sequence

Emphasis of this study is on the development of the dominant systematic extension fractures, including veins and joints, and occasionally associated small-displacement shear fractures or faults. Observations and data to constrain timing of this fracturing include relative timing relationships between structures in the exposure,

and association of these structures with recognized tectonic events that are well-characterized in the region. Laramide and Basin and Range deformation features are well documented in the Sierra del Carmen (Moustafa, 1988; Turner et al., 2011) and at Ernst Tinaja (Ferrill et al., 2016).

Recognized Laramide deformation features include contractional folds, thrust faults, and tectonic stylolites that collectively accommodated NE-SW directed shortening in response to NE-SW directed maximum principal stress, σ_1 . Where the systematic NW-SE striking extension fractures – the focus of this investigation – interact with thrust faults, they cut the thrust faults, indicating extension fracturing after thrust faulting (Ferrill et al., 2016). Similarly, where the NW-SE striking extension fractures interact with the tectonic stylolites, they cut the stylolite teeth or locally show dilational reactivation of the stylolites, thus indicating extension fracturing after stylolite formation. Furthermore, the NW-SE striking opening mode fractures indicate NE-SW directed minimum principal stress direction (σ_3), which is consistent with the regional Basin and Range extension direction. We deliberately avoided running scanline surveys through contractional folds to avoid any local fold-related extension fracturing, for example related to outer-arc extension in competent limestone beds. All of our scanlines were collected from consistently dipping homoclinal beds.

Laramide contractional deformation of these rocks is likely to have occurred at burial depths of ~2 km or less (based on overburden thickness estimates from measured sections in Maxwell et al., 1967). Subsequent Basin and Range extension of these rocks

may have initiated while the rocks were at or near maximum burial of ~2 km (related to sedimentary burial and tectonic thickening during the Laramide deformation), and continued during tectonic and erosional exhumation related to Basin and Range extension with progressively decreasing overburden.

4. Methods

4.1. Mechanical stratigraphy

A mechanical rebound data set was collected for the entire Ernst Tinaja section using an N-type Schmidt hammer (Katz et al., 2000; Aydin and Basu, 2005) to characterize the relative competence of the present-day mechanical stratigraphic layers (Ferrill and Morris, 2008). Compared to other approaches for obtaining rock mechanics data (such as scratch test, indirect or Brazilian tensile test, unconfined and confined compression test), the Schmidt Hammer provides a quick and inexpensive proxy for rock mechanics data. The rebound analysis used in this work followed the approach described by Morris et al. (2009) and Ferrill et al. (2011, 2012a, 2012b). To summarize those studies (i) measurements were taken on subvertical rock faces to eliminate the need to correct for gravity effect, and (ii) each measurement location consisted of a minimum of 10 rebound measurements within an area of approximately 25 cm² with care to stay within the same mechanical layer. The N-type Schmidt hammer used in this work does not allow accurate and precise measurement of very weak rock where rebound (R) values are less than 10. Values recorded in the field that are less

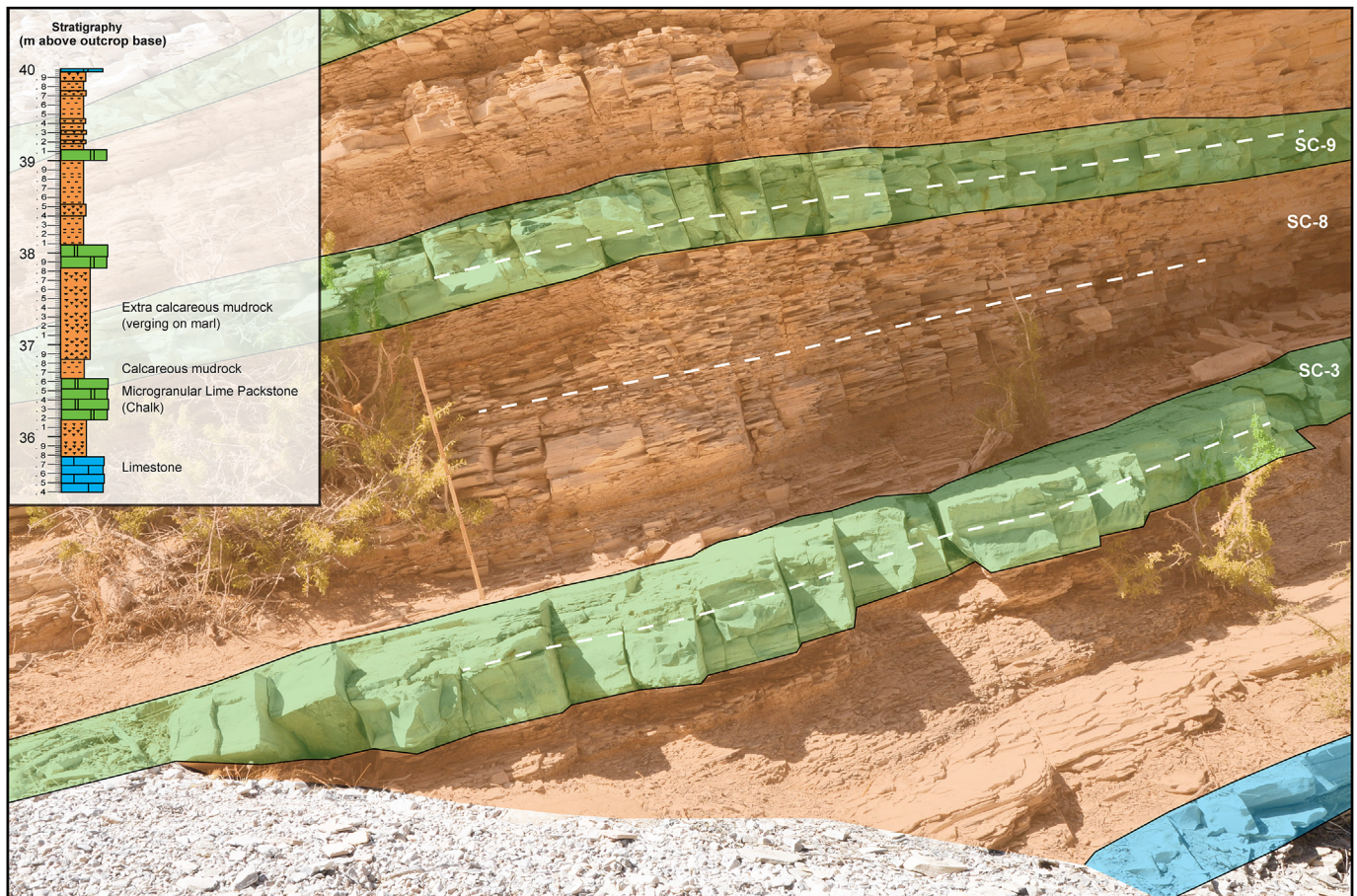


Fig. 2. Annotated field photograph showing examples of the fracture scanlines. Ruler (perpendicular to layering) is 1 m long for scale and photo was taken with view to the north-northwest.

than 10 were treated as having a value of 5 when averaged to determine bed average R values. We present the results in terms of rebound value R, which has been correlated to unconfined compressive strength and Young's modulus through laboratory testing (e.g., Katz et al., 2000; Aydin and Basu, 2005). Although published correlations differ in detail, rebound values between 20 and 55 generally correlate with an unconfined compressive strength range of ~5.0–40 MPa and Young's moduli of 2.0–15 GPa. We use the term "competence" to express the ability of a rock to resist deformation (Ferrill and Morris, 2008). Rock properties are expected to have been modified, commonly weakening the rock, as a result of unloading and erosion. Notwithstanding the limitations of Schmidt hammer rebound values (see for example, Morris et al., 2009) and influences of weathering, we interpret the R-value profiles as reflecting the relative competence between rock layers from one location to another.

4.2. Fracture characterization

Here we use the term fracture to include any discontinuity in the rock where cohesion has been lost via brittle deformation processes, and includes: (i) opening-mode extension fracture (barren or vein filled); (ii) fault or shear fracture where the two sides have been displaced with respect to each other and parallel to the fracture surface (barren or vein filled); (iii) contractional stylolite; (iv) reactivated stylolite as an opening-mode extension fracture (barren or vein filled) with no visible shear displacement. We observe calcite as the mineral fill for the veins at Ernst Tinaja.

Scanline surveys were conducted parallel to dip along the center lines of beds (Fig. 2). Every fracture that intersected along the

profile was measured for strike and dip, trace length or lateral penetration (where top of bed pavements permitted measurement), penetration distance upward and downward to fracture tips, aperture (separation of fracture walls measured perpendicular to plane of fracture), and vein fill (if present). While opening-mode fracture aperture was recorded, we do not consider these values to be particularly useful for purposes of fracture network characterization due to unloading related dilation and weathering. Surface unloading and near-surface dissolution has altered the apparent fracture aperture from its likely original character, and some soluble (e.g., calcite) fracture filling material that may have been present may have been removed by dissolution. Scanline lengths ranged from 2.5 to 5.0 m. Selection of beds for scanline surveys was intended to characterize a representative range of rock types (mudrock, chalk, and limestone) and a range of bed thicknesses. Also, due to the dip of the beds, shorter scanlines were more accessible. Care was taken not to choose a scanline that was near or crossed large folds or faults so that the influence of the larger structure would be minimal.

5. Results

5.1. Mechanical stratigraphy

For these rocks, clay mineralogy drives whether the rock type is incompetent, as is the case for the clay-rich mudrocks, or whether it is competent, as is the case for clay-poor limestones and chinks. Results from 30 X-ray diffraction (XRD) bulk composition and clay analyses show that the mudrocks have a high clay content (15–90% clay minerals) and the chalk and limestone beds have low clay

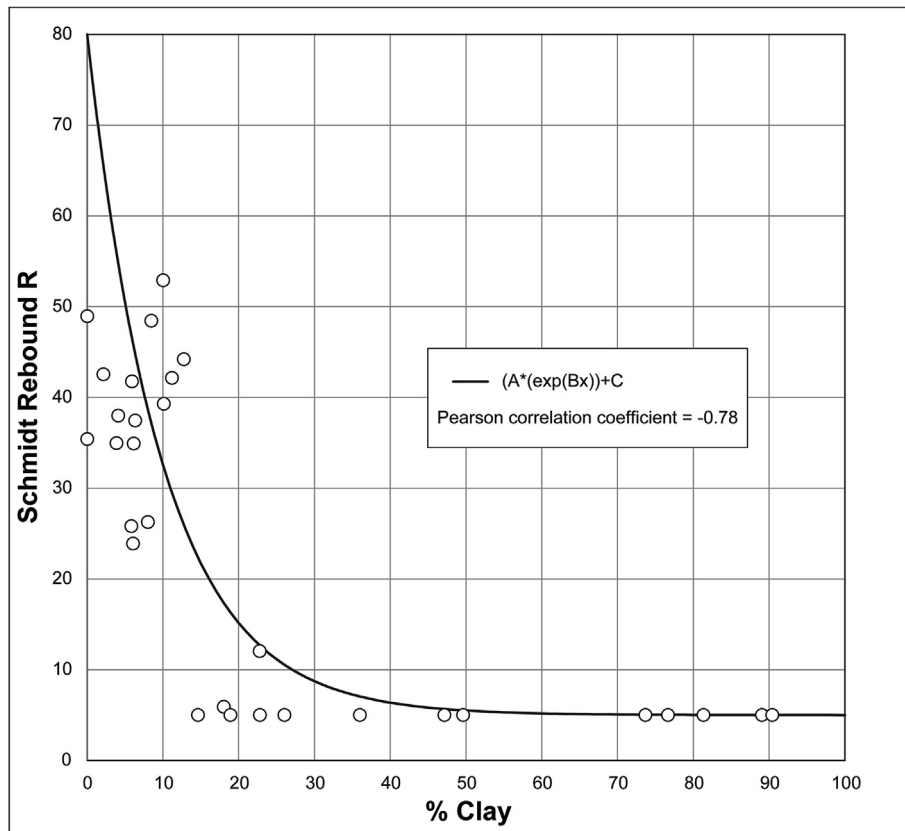


Fig. 3. Plot and empirical relationship between Schmidt rebound (average R) values and measured percent clay. Heavy line is an exponential-fit correlation, where $A = 75$, $B = -0.1$, and $C = 5$. Using Eq. (1) in text, the Pearson correlation coefficient (r) was calculated to be -0.78 . Rebound measurements were conducted in the present study (see text); Percent clay was determined from XRD analysis (total weight).

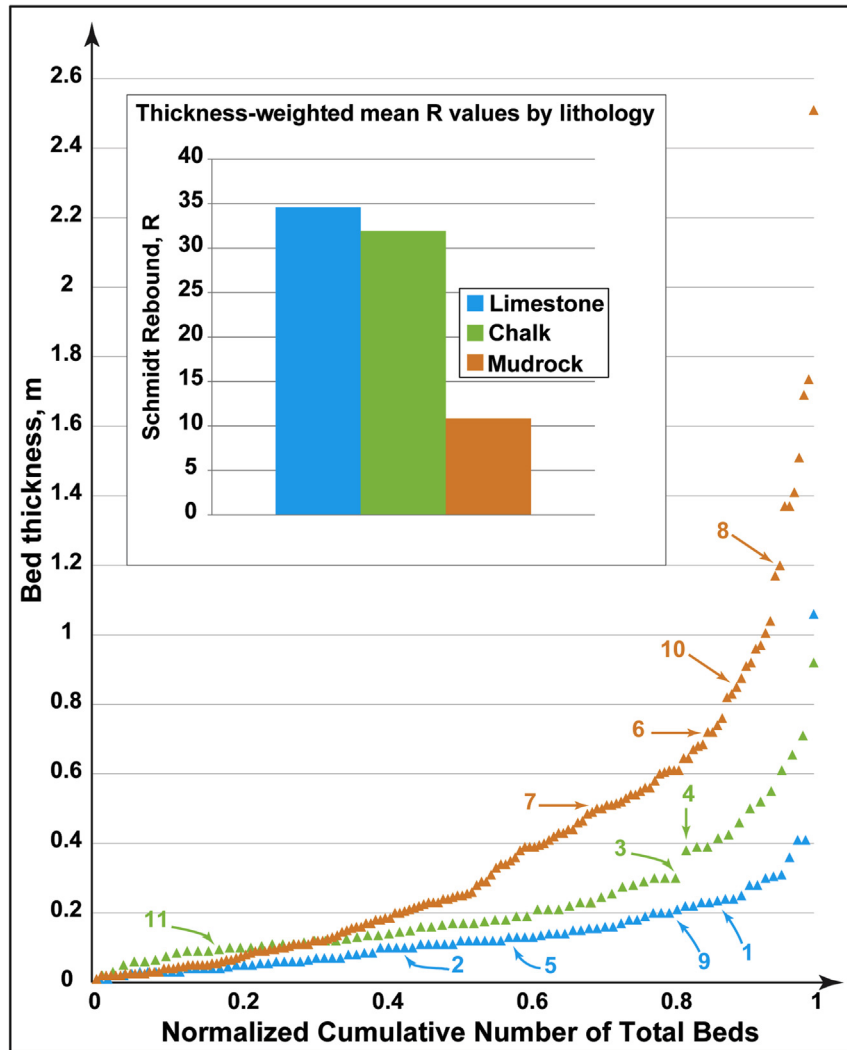


Fig. 4. Plot showing all beds in the measured lithostratigraphic section. Triangles represent each bed thickness in the section ordered from thin to thick and colored by lithology. Normalized cumulative number = n/n_{total} . Number and arrow denotes each scanline survey bed. Inset shows average rebound value for each lithology.

content (0–12% clay minerals). A strong inverse correlation is observed in a plot of rebound value versus percent clay content (Fig. 3). Samples with $\geq 15\%$ clay have the lowest average rebound values (all < 15), whereas layers with $< 12\%$ clay have R values of > 24 . Using the Pearson correlation equation, a coefficient (r) of -0.78 was calculated (Fig. 3).

$$r = \frac{N \sum xy - (\sum x)(\sum y)}{\sqrt{[N \sum x^2 - (\sum x)^2][N \sum y^2 - (\sum y)^2]}} \quad (1)$$

Where:

- N = number of pairs of scores
- $\sum xy$ = sum of the products of paired scores
- $\sum x$ = sum of x scores
- $\sum y$ = sum of y scores
- $\sum x^2$ = sum of squared x scores
- $\sum xy^2$ = sum of squared y scores

Mudrock forms the thickest beds with 57% of all the mudrock layers in the stratigraphic section greater than 0.20 m thick and 45% greater than 0.30 m thick (Fig. 4). Limestone and chalk tend to form

thinner beds with 80% of limestone layers and 60% of chalk layers less than 0.20 m thick, and only 20% of chalk and 7% of limestone beds exceeding 0.30 m in thickness (Fig. 4).

5.2. Fracture characterization

Eleven dip-parallel scanline surveys were conducted in representative mudrock, limestone, and chalk beds (designated 1 through 11 in Table 1, Table 2, and Fig. 5). The scanline orientation was selected to capture the dominant opening-mode extension fracture set (approximately north-northwest striking and bed-perpendicular or at high angle to bedding). In addition, the scanlines were selected so that the influence from larger structures (tectonic folds, normal faults, and thrust faults) would be minimal. The majority of fractures that each scanline encountered were opening-mode extension fractures both barren (48%) and vein filled (44%) and smaller numbers of other fracture types (Table 2). While fracture strike orientations are nearly identical for all scanlines, fracture dip tends to be lower in the mudrocks and higher in the chalks and limestones (Fig. 5). Mean fracture spacing and bed thickness ratios were determined from the observed data for each scanline. For a particular lithology, mean fracture spacing tends to

Table 1
Fracture scanline summary.

Scanline #	Lithology	Stratigraphic Height (m)	Rebound	Bed Thickness (m)	Mean Spacing (m)	Spacing/Thickness Ratio	CV ^a
Line 3	Chalk	36.50	37.65	0.34	0.20	0.58	0.49
Line 4	Chalk	52.80	49.00	0.37	0.33	0.89	0.60
Line 11	Chalk	54.30	27.10	0.10	0.08	0.83	0.98
Line 1	Limestone	3.00	42.55	0.22	0.27	1.23	0.69
Line 2	Limestone	6.90	41.20	0.10	0.13	1.33	0.65
Line 5	Limestone	7.75	37.45	0.13	0.10	0.74	0.62
Line 9	Limestone	37.95	37.40	0.33	0.10	0.31	0.65
Line 6	Mudrock	7.30	7.55	0.70	0.07	0.11	0.69
Line 7	Mudrock	3.60	16.18	0.55	0.13	0.24	0.89
Line 8	Mudrock	37.20	7.02	1.24	0.12	0.09	0.73
Line 10	Mudrock	53.40	11.50	0.84	0.21	0.25	0.58

^a CV = coefficient of variation and is standard deviation of fracture spacing divided by mean fracture spacing.

Table 2
Fracture type summary.

Scanline #	Opening-Mode Extension Fracture		Fault		Stylolite	Reactivated Stylolite	
	Barren	Vein Filled	Barren	Vein Filled		Barren	Vein Filled
Line 1	12.5%	81.3%	0.0%	6.3%	0.0%	0.0%	0.0%
2	32.3%	51.6%	0.0%	0.0%	9.7%	6.5%	0.0%
3	26.3%	57.9%	5.3%	0.0%	0.0%	10.5%	0.0%
4	25.0%	62.5%	0.0%	0.0%	12.5%	0.0%	0.0%
5	48.8%	43.9%	0.0%	0.0%	2.4%	2.4%	2.4%
6	100.0%	0.0%	0.0%	0.0%	0.0%	0.0%	0.0%
7	53.8%	26.9%	0.0%	0.0%	19.2%	0.0%	0.0%
8	100.0%	0.0%	0.0%	0.0%	0.0%	0.0%	0.0%
9	36.0%	60.0%	0.0%	0.0%	0.0%	0.0%	4.0%
10	11.1%	88.9%	0.0%	0.0%	0.0%	0.0%	0.0%
11	9.7%	83.9%	0.0%	6.5%	0.0%	0.0%	0.0%
Total	47.8%	44.4%	0.4%	1.1%	3.7%	1.9%	1.1%

increase with bed thickness (Fig. 6A). The relationships are similar for limestone (mean spacing/thickness ratio = 0.90) and chalk beds (mean spacing/thickness ratio = 0.77), but dramatically lower for mudrock (mean spacing/thickness ratio = 0.17). Fracture spacing/bed thickness ratio tends to be higher for beds with R greater than 20 (Fig. 6B), but there is not a good statistical fit for this relationship.

The regularity of fracture spacings was quantified by using the coefficient of variation (Cv; Table 1) of the population of fracture spacings, whereby the standard deviation of the population of spacings is divided by the arithmetic mean (e.g., Kagan and Jackson, 1991; Gillespie et al., 1999; Supak et al., 2006). For this type of analysis, the greater the value of Cv, the more irregular the fracture spacing. For example, a Cv value of 1 is expected for a Poissonian distribution of spacings and signifies spacings between randomly positioned fractures (Gillespie et al., 1999). Accordingly, fractures that are more clustered than expected for randomly arranged fractures will have Cv that is greater than 1, and those having a more uniform spacing will have Cv less than 1 (Gillespie et al., 1999). The fractures at Ernst Tinaja have Cv values consistently <1. For chalk and mudrock beds, the Cv values range from 0.49 up to 0.98 whereas are the limestone beds are much more consistent (0.62–0.69).

The Ernst Tinaja outcrop provided excellent exposure for vertical fracture penetration to be examined. The penetration heights were measured from the center of the bed upward and downward using the lithologic bed boundary as reference. A ratio of height of fracture penetration versus distance from center of the bed to the bed boundary was determined for each fracture measured and was plotted against stratigraphic bed thickness (Fig. 7). Results of this analysis show that bed-perpendicular fractures within chalk and limestone beds commonly penetrate the entire bed thickness and

extend into the adjacent mudrock beds (Fig. 7). In contrast, fractures in the mudrock beds rarely penetrate to or beyond the bed boundaries into the adjacent carbonate beds. Compared to the Hooker et al. (2013) fracture height classification, fractures in the mudrock layers tend to exist within the layer or are top bounded. Fractures in the chalk and limestone layers exhibit both bed-bounded and unbounded behavior.

6. Discussion

In addition to lithology and bed thickness, bed-to-bed transitions are a key element to characterizing mechanical stratigraphy for the purpose of understanding and predicting fractures. Numerical modeling and outcrop studies (Helgeson and Aydin, 1991; Cooke and Underwood, 2001; Laubach et al., 1998; Gillespie et al., 1999; Hooker et al., 2013; Chang et al., 2015; Ferrill et al., 2017) show that the interface shear strength is a critical factor with respect to the development of mechanical discontinuities at layer boundaries and the ability to terminate bed-perpendicular fracture propagation versus continued fracture propagation and increasing fracture penetration. Low shear strength and poorly bonded interfaces help terminate fracture propagation whereas high shear strength and well bonded interfaces allow fractures to grow across bed interfaces. High shear strength, well bonded interfaces correlate with gradual lithological and mineralogical transitions, and low shear strength, poorly bonded interfaces correlate with abrupt lithological and mineralogical transitions between beds. Thus, the abruptness of lithological transitions is an important indicator of the interface strength and the ability or inability to terminate a propagating fracture (Cooke and Underwood, 2001; Mandl, 2005). In the Ernst Member of the Boquillas Formation at Ernst Tinaja, we

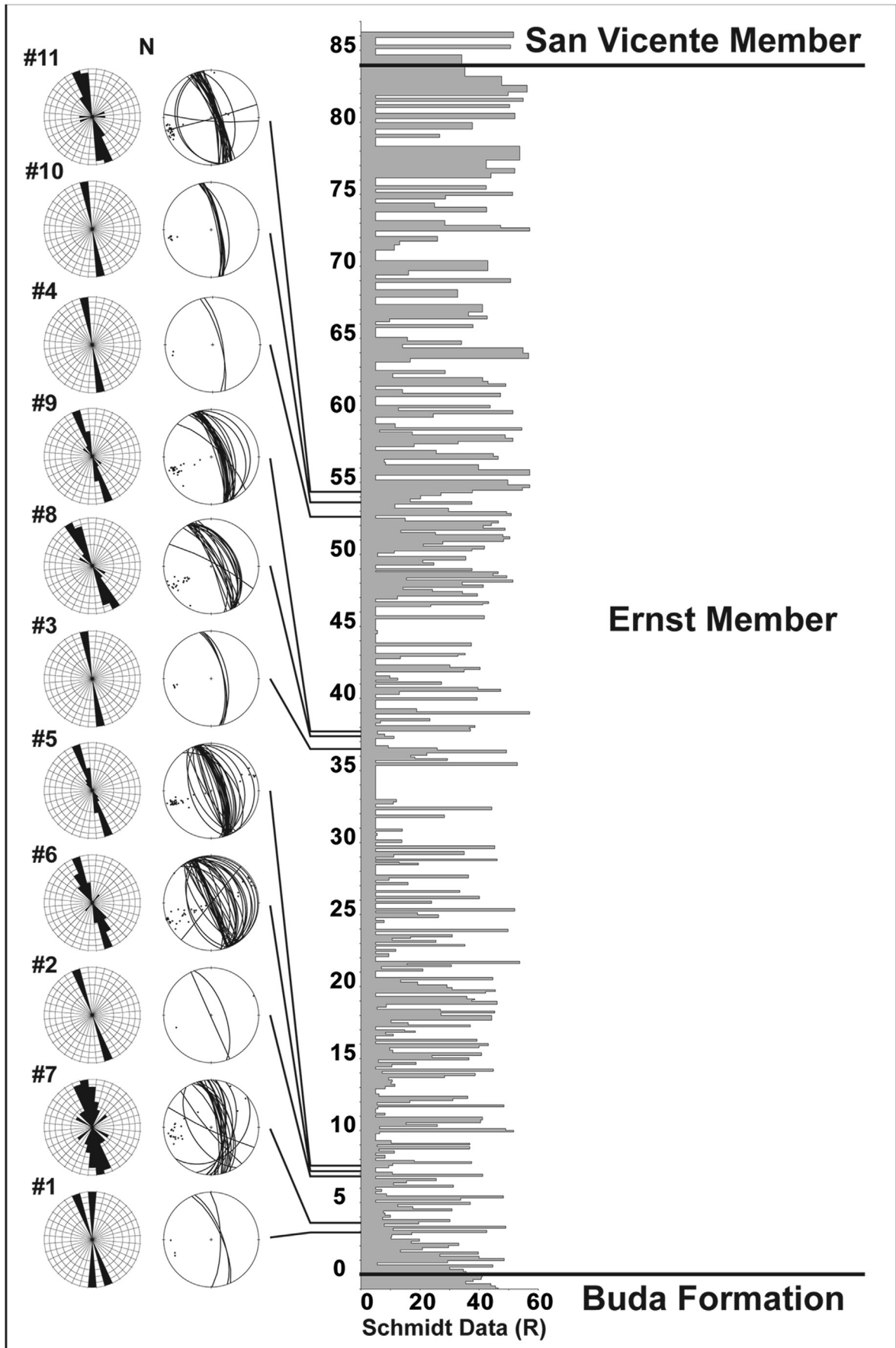


Fig. 5. Number-weighted rose diagrams and equal-area, lower hemisphere projections representing all fracture data for each of the 11 scanline datasets. Mechanical stratigraphic (Schmidt rebound, R) section for full Ernst Member at Ernst Tinaja with lines showing the stratigraphic height for each scanline. The vertical scale represents stratigraphic position in meters from base of section.

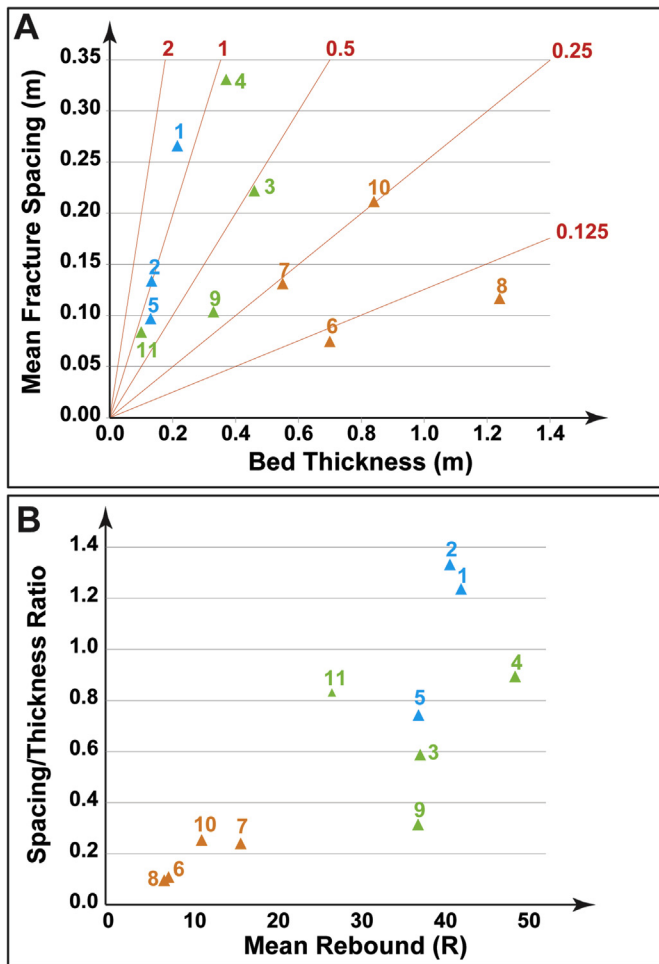


Fig. 6. (A) Mean fracture spacing plotted versus bed thickness. Red lines represent different thickness versus spacing ratios. (B) Fracture spacing/bed thickness ratio plotted versus mean rebound. Data points are labeled by scanline numbers 1 through 11 and colored by lithology (blue = limestone, green = chalk, and orange = mudrock).

observe (i) abrupt limestone to mudrock transitions, and (ii) gradual chalk to mudrock transitions. The hydrodynamically winnowed limestone beds are more likely to exhibit abrupt bed transitions with adjacent mudrocks. By contrast, gradual bed transitions are more often found within pelagic sections, likely to have been deposited below storm wave base where lithologic composition is dictated by the relative abundance of planktonic foraminifera and clay minerals that reach the ocean floor. Furthermore, in contrast to some other studies (Gillespie et al., 1999; Hooker et al., 2013), we found that both vein-filled and barren fractures show similar behavior with respect to penetration height and influence of the mechanical boundaries (Fig. 6).

The higher mean fracture spacing/bed thickness ratio for limestone and chalk versus mudrock (Table 1) may be related to the greater ductility or lower Young's modulus of the mudrock compared with limestone and chalk. Weaker rock suppresses fracture initiation and internal clay-rich laminations of low shear strength within mudrock beds that may inhibit fracture propagation across layering (Price, 1966; Ellis et al., 2012).

The results presented here show distinctly different fracture spacing and penetration characteristics for the more competent limestone and chalk beds versus the incompetent mudrock beds. Although the fracture literature includes many papers documenting fracture spacing versus bed thickness relationships, these

studies most commonly focus on the more competent beds where fracture networks are often better developed and the beds are relatively thin (e.g., see compilation in McGinnis et al., 2015). For example, positive correlations between fracture spacing and bed thickness, or inverse relationships between fracture frequency and bed thickness, have been documented (e.g., Harris et al., 1960; Price, 1966; McQuillan, 1973; Ladeira and Price, 1981; Corbett et al., 1987; Huang and Angelier, 1989; Narr and Suppe, 1991; Nelson, 2001; Ogilvie et al., 2006). Deciding when and where these relationships should be applied to subsurface fracture prediction can be a problem. In most cases, site-specific relationships are difficult to determine because relevant subsurface data is not available or is too limited. Our results suggest that different relationships need to be applied to accurately predict fracturing in mechanically layered rocks. Measuring mechanical properties such as Young's modulus or using proxies such as mechanical rebound (Schmidt Hammer in outcrop and Bambino for core) and mineralogic composition (XRD and XRF) to characterize mechanical stratigraphy should be a first-order exercise and can be used to select or adjust fracture relationships (e.g., spacing versus thickness, penetration heights, bed interfaces) at the formation scale down to the bed scale. Using spacing versus thickness ratios from this study, one could assume that for generally competent rocks a ratio 0.31–1.33 might be used. For less competent rocks, a ratio of 0.09–0.25 might be more reasonable.

The bed scale control on fracture heights illustrated in this study shows that mechanical stratigraphy controls fracture system development at a smaller scale than can be discerned from modern subsurface technologies such as seismic reflection data or standard wireline log data, but the mechanical stratigraphy can be observed at this scale in core and in high-frequency wireline logs. Given that fracture spacing dimensions are typically wider than core, a thorough understanding of the bed-scale mechanical stratigraphy along with site-specific observations from all available datasets can provide a baseline understanding of the factors that control fracture development in the subsurface. Focusing on these controls can increase the usefulness and reduce the uncertainty of fracture models as they pertain to subsurface fracture characterization.

7. Conclusions

Analysis of a range of fracture types (opening-mode fractures, veins, stylolites, and small displacement shear fractures) from a series of Cretaceous limestone, chalk, and mudrock beds demonstrates that there is strong influence of lithology and mechanical bed character on the bed-parallel spacing and bed-perpendicular penetration of fractures. Fracture spacing in limestone and chalk beds shows a strong correlation with bed thickness with spacing/thickness ratios of 0.31–1.33. In limestone and chalk, fractures generally penetrate the entire bed thickness and extend into adjacent mudrocks. In contrast, fracture spacing in mudrock beds shows a poorer correlation with bed thickness and a significantly smaller spacing/thickness ratio of 0.09–0.25. Fractures in mudrock beds typically terminate within mudrock beds. Consequently, the overall natural fracture connectivity through the mechanically layered sequence generally is poor.

Induced hydraulic fracturing is likely to reactivate and link the natural fracture networks. Variability in well performance may be strongly influenced by the mechanical layering and related influence on fracturing in fine grained sedimentary strata. These results also have direct importance and relevance to groundwater and contaminant movement in the subsurface, and containment of waste in fine-grained, low-permeability strata. Fracture prediction techniques, including discrete fracture network simulations, need

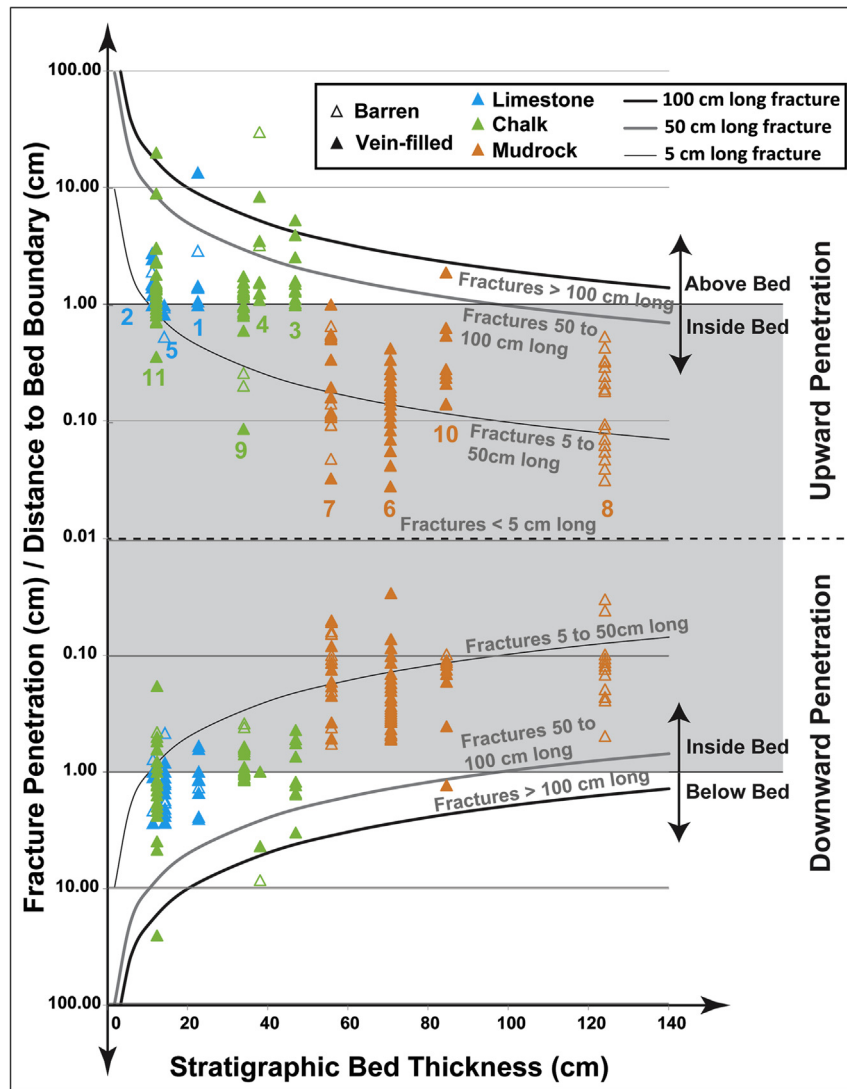


Fig. 7. This plot shows normalized fracture penetration versus stratigraphic bed thickness. Colored triangles represent each fracture measured for vertical penetration (upward and downward from the middle of each measured bed) along the scanline for a specific lithology and at a particular stratigraphic height. The shaded area represents the inside of each bed surveyed. The scanline number is labeled. Curves represent total fracture length for a given penetration and bed thickness.

to consider this thin bed-scale control on fracture heights, and the strong lithologic control on fracture spacing.

Acknowledgements

We appreciate Big Bend National Park allowing us to conduct this research under research permit # BIBE-2013-SCI-0033. We thank Zach Sickmann, Marques Miller, and Mary-Katherine Todt for assistance in the field, and Erich De Zoeten and Michael Bentz for assistance with data reduction. Financial support for this work was provided through Southwest Research Institute's Eagle Ford joint industry project, funded by Anadarko Petroleum Corporation, BHP Billiton, Chesapeake Energy Corporation, ConocoPhillips, Eagle Ford TX LP, EP Energy, Hess Corporation, Marathon Oil Corporation, Murphy Exploration and Production Company, Newfield Exploration Company, Pioneer Natural Resources, and Shell. We thank the staff of these sponsor companies for the interaction and constructive feedback. In addition, we thank Peter Hennings, Terry Engelder, David Sanderson, Steve Laubach, Carlos Fernandez, and Toru Takeshita for their very helpful reviews.

References

- Aydin, A., Basu, A., 2005. The Schmidt hammer in rock material characterization. *Eng. Geol.* 81, 1–14.
- Chang, X., Shan, Y., Zhang, Z., Tang, C., Ru, Z., 2015. Behavior of propagating fracture at bedding interface in layered rocks. *Eng. Geol.* 197, 33–41.
- Cooke, M.L., Underwood, C.A., 2001. Fracture termination and step-over at bedding interfaces due to frictional slip and interface opening. *J. Struct. Geol.* 23, 223–238.
- Corbett, K., Friedman, M., Spang, J., 1987. Fracture development and mechanical stratigraphy of Austin Chalk. *Tex. AAPG Bull.* 71, 17–28.
- Ellis, M.A., Laubach, S.E., Eichhubl, P., Olson, J.E., Hargrove, P., 2012. Fracture development and diagenesis of Torridon Group Applecross Formation, near an Teallach, NW Scotland: millennia of brittle deformation resilience? *J. Geol. Soc. London* 169, 297–310.
- Engelder, T., 1985. Loading paths to joint propagation during a tectonic cycle: an example from the Appalachian Plateau, U.S.A. *J. Struct. Geol.* 7, 459–476.
- English, J.M., 2012. Thermomechanical origin of regional fracture systems. *AAPG Bull.* 96, 1597–1625.
- Erdlac Jr., R.H., 1994. Laramide paleostress trajectories from stylolites in the Big Bend region. In: Laroche, T.M., Viveiros, J.J. (Eds.), *Structure and Tectonics of the Big Bend and Southern Permian Basin*. West Texas Geological Society 1994 Field Trip Guidebook, Publication, 94–95, pp. 165–187.
- Ferrill, D.A., Morris, A.P., 2008. Fault zone deformation controlled by carbonate mechanical stratigraphy, Balcones fault system. *Tex. AAPG Bull.* 92, 359–380.
- Ferrill, D.A., Morris, A.P., McGinnis, R.N., Smart, K.J., Ward, W.C., 2011. Fault zone

- deformation and displacement partitioning in mechanically layered carbonates: the Hidden Valley fault, central Texas. *AAPG Bull.* 95, 1383–1397.
- Ferrill, D.A., McGinnis, R.N., Morris, A.P., Smart, K.J., 2012a. Hybrid failure: field evidence and influence on fault refraction. *J. Struct. Geol.* 42, 140–150.
- Ferrill, D.A., Morris, A.P., McGinnis, R.N., 2012b. Extensional fault-propagation folding in mechanically layered rocks: the case against the frictional drag mechanism. *Tectonophysics* 576–577, 78–85.
- Ferrill, D.A., McGinnis, R.N., Morris, A.P., Smart, K.J., Sickmann, Z.T., Bentz, M., Lehrmann, D., Evans, M.A., 2014. Control of mechanical stratigraphy on bed-restricted jointing and normal faulting: Eagle Ford Formation, south-central Texas. *U.S.A. AAPG Bull.* 98, 2477–2506.
- Ferrill, D.A., Morris, A.P., McGinnis, R.N., Smart, K.J., Wigginton, S.S., Hill, N.J., 2017. Mechanical stratigraphy and normal faulting. *J. Struct. Geol.* 94, 275–302.
- Ferrill, D.A., Morris, A.P., Wigginton, S.S., Smart, K.J., McGinnis, R.N., Lehrmann, D., 2016. Deciphering thrust fault nucleation and propagation and the importance of footwall synclines. *J. Struct. Geol.* 85, 1–11.
- Gale, J.F.W., Laubach, S.E., Olson, J.E., Eichhubl, P., Fall, A., 2014. Natural fractures in shale: a review and new observations. *AAPG Bull.* 98, 2165–2216.
- Gillespie, P.A., Johnston, J.D., Loriga, M.A., McCaffrey, K.L.W., Walsh, L.L., Watterson, L., 1999. Influence of layering on vein systematics in line samples. In: McCaffrey, K.J.W., Lonergan, L., Wilkinson, J.J. (Eds.), *Fractures, Fluid Flow and Mineralization*. Geol. Soc., London, 155, pp. 35–56.
- Gillespie, P., Walsh, J.J., Watterson, J., Bonson, C.G., Manzocchi, T., 2001. Scaling relationships of joint and vein arrays from the Burren, Co. Clare Ireland. *J. Struct. Geol.* 23, 183–201.
- Groshong Jr., R.H., 2006. *3-D Structural Geology*. Springer-Verlag, Heidelberg, 400 p.
- Gross, M.R., 1993. The origin and spacing of cross joints: examples from the Monterey Formation, Santa Barbara coastline, California. *J. Struct. Geol.* 15, 737–751.
- Hancock, P.L., 1985. Brittle microtectonics: principles and practice. *J. Struct. Geol.* 7, 437–457.
- Harris, J.F., Taylor, G.L., Walper, J.L., 1960. Relation of deformational features in sedimentary rocks to regional and local structures. *AAPG Bull.* 44, 1853–1873.
- Helgeson, D.E., Aydin, A., 1991. Characteristics of joint propagation across layer interfaces in sedimentary rocks. *J. Struct. Geol.* 13, 897–991.
- Huang, Q., Angelier, J., 1989. Fracture spacing and its relation to bed thickness. *Geol. Mag.* 126, 355–362.
- Hooker, J.N., Laubach, S.E., Marrett, R., 2013. Fracture-aperture sized frequency, spatial distribution, and growth processes in strata-bounded and non-strata-bounded fractures, Cambrian Mesón Group, NW Argentina. *J. Struct. Geol.* 54, 54–71.
- Kagan, Y.Y., Jackson, D.D., 1991. Long-term earthquake clustering. *Geophys. J. Int.* 104, 117–133.
- Katz, O., Reches, Z., Roegiers, J.C., 2000. Evaluation of mechanical rock properties using a Schmidt Hammer. *Int. J. Rock Mech. Min. Sci.* 37, 723–728.
- Ladeira, F.L., Price, N.J., 1981. Relationship between fracture spacing and bed thickness. *J. Struct. Geol.* 3, 179–183.
- Laubach, S.E., Marrett, R., Olson, J.E., Scott, A.R., 1998. Characteristics and origins of coal cleat: a review. *Int. J. Coal Geol.* 35, 175–207.
- Laubach, S.E., Olson, J.E., Gross, M.R., 2009. Mechanical and fracture stratigraphy. *AAPG Bull.* 93, 1413–1426.
- Laubach, S.E., Eichhubl, P., Hilgers, C., Lander, R.H., 2010. Structural diagenesis. *J. Struct. Geol.* 32, 1866–1872.
- Lehman, T.L., 1991. Sedimentation and tectonism in the Laramide Tornillo Basin of west Texas. *Sediment. Geol.* 75, 9–28.
- Maler, M.O., 1990. Dead Horse Graben: a west Texas accommodation zone. *Tectonics* 9, 1357–1368.
- Mandl, G., 2005. *Rock Joints – the Mechanical Genesis*, vol. 221. Springer.
- McQuillan, H., 1973. Small-scale fracture density in Asmari Formation of southwest Iran and its relation to bed thickness and structural setting. *AAPG Bull.* 57, 2367–2385.
- Maxwell, R.A., Lonsdale, J.T., Hazzard, R.T., Wilson, J.A., 1967. *Geology of the Big Bend National Park, Brewster County, 6711*. University of Texas at Austin, Bureau of Economic Geology Publication, Texas, p. 320.
- McGinnis, R.N., Ferrill, D.A., Smart, K.J., Morris, A.P., Higuera-Diaz, C., Prawica, D., 2015. Pitfalls of using entrenched fracture relationships. Fractures in bedded carbonates of the hidden valley fault zone, canyon lake gorge, comal county, Texas. *AAPG Bull.* 99, 2221–2245.
- McGinnis, R.N., Ferrill, D.A., Morris, A.P., Smart, K.J., 2016. Insight on mechanical stratigraphy and subsurface interpretation. In: Krantz, B., Ormand, C., Freeman, B. (Eds.), *3-D Structural Interpretation: Earth, Mind, and Machine*, vol. 111. *AAPG Memoir*, pp. 111–120.
- Morris, A.P., Ferrill, D.A., McGinnis, R.N., 2009. Mechanical stratigraphy and faulting in Cretaceous carbonates. *AAPG Bull.* 93 (11), 1459–1470.
- Moustafa, A.R., 1988. *Structural Geology of Sierra del Carmen, Trans-Pecos Texas. 1: 48,000 scale geologic map: Geologic Quadrangle Map, 54*, Bureau of Economic Geology, The University of Texas at Austin, Austin, Texas.
- Narr, W., 1991. Fracture density in the deep subsurface: techniques with application to Point Arguello Oil Field. *AAPG Bull.* 75, 1300–1323.
- Narr, W., Suppe, J., 1991. Joint spacing in sedimentary rocks. *J. Struct. Geol.* 13, 1037–1048.
- Narr, W., Schechter, D.W., Thompson, L.B., 2006. *Naturally Fractured Reservoir Characterization*. SPE, Richardson, Texas, 112 p.
- Nelson, R.A., 2001. *Geologic Analysis of Naturally Fractured Reservoirs*, second ed. Gulf Professional Publishing, Boston, Massachusetts, 332 p.
- Ogilvie, S.R., Isakov, E., Glover, P.W.J., 2006. Fluid flow through rough fractures in rocks. II: a new matching model for rough rock fractures. *Earth Planet. Sci. Lett.* 241, 454–465.
- Olson, J.E., Laubach, S.E., Lander, R.H., 2009. Natural fracture characterization in tight gas sandstones: integrating mechanics and diagenesis. *AAPG Bull.* 93, 1535–1549.
- Ortega, O.O., Gale, J.F.W., Marrett, R., 2010. Quantifying the diagenetic and stratigraphic controls on fracture intensity in platform carbonates: an example from the Sierra Madre Oriental, northeast Mexico. *J. Struct. Geol.* 32, 1943–1959.
- Price, N.J., 1966. *Fault and Joint Development in Brittle and Semi-brittle Rock*. Pergamon Press, p. 176.
- Ramsay, J.G., 1967. *Folding and Fracturing of Rocks*. McGraw Hill, New York, 568p.
- Ramsay, J.G., Huber, M.I., 1987. *The Techniques of Modern Structural Geology, 2. Folds and Fractures*. Academic Press, London, pp. 561–594.
- Supak, S., Bohnenstiehl, D.R., Buck, W.R., 2006. Flexing is not stretching: an analogue study of flexure-induced fault populations. *Earth Planet. Sci. Lett.* 246, 125–137.
- Turner, K.J., Berry, M.E., Page, W.R., Lehman, T.M., Bohannon, R.G., Scott, R.B., Miggins, D.P., Budahn, J.R., Cooper, R.W., Drenth, B.J., Anderson, E.D., Williams, V.S., 2011. *Geologic Map of Big Bend National Park*. U. S. Geological Survey Scientific Investigations Map 3142, scale 1, Texas, p. 84, 75,000, pamphlet.